Enhanced thermal and fire retardancy properties of polypropylene reinforced with a hybrid graphene/glass-fibre filler

Dimitrios G. Papageorgiou[a]*, Zoe Terzopoulou[b], Alberto Fina[c], Fabio Cuttica[c], George Z. Papageorgiou[d], Dimitrios N. Bikiaris[b], Konstantinos Chrissafis[e], Robert J. Young[a], Ian A. Kinloch[a*]

[a] *School of Materials and National Graphene Institute, University of Manchester, Oxford Road, M13 9PL, United Kingdom*

[b] *Laboratory of Polymer Chemistry and Technology, Department of Chemistry, Aristotle University of Thessaloniki, GR-541 24, Thessaloniki, Greece*

[c] *Dipartimento di Scienza Applicata e Tecnologia, Politecnico di Torino, 15121 Alessandria, Italy*

[d] *Chemistry Department, University of Ioannina, P.O. Box 1186, 45110, Ioannina, Greece*

[e] *Solid State Physics Section, Physics Department, Aristotle University of Thessaloniki, 541 24 Thessaloniki, Greece*

Abstract

The thermal stability and flame retardancy properties of polypropylene (PP) nanocomposites containing graphene nanoplatelets (GNPs), glass fibres (GFs) or a hybrid mixture of the two fillers were investigated. The GNPs enhanced the thermal stability of the nanocomposites by at least 48 ^{o}C as a result of the nanoconfinement of the polypropylene chains and the prevention of the emission of the gaseous molecules during decomposition. Pyrolysis combined with gas chromatography and mass spectroscopy showed that the decomposition mechanism of the polymer was not altered by the presence of the nanofillers and the alkenes that comprised of 3*n* carbon atoms were the main degradation products. Cone calorimetry tests revealed a significant delay of the ignition under

irradiation with the addition of GNPs to the PP. Furthermore, the GNPs lowered the combustion rate of the PP due to the formation of a carbonaceous protective layer that acted as a barrier to heat and mass transfer. The lightweight materials prepared show promising results for applications where high thermal stability along with fire retardancy are a prerequisite, such as parts for vehicles or aircraft.

Keywords: polypropylene; graphene nanoplatelets; glass fibres; fire retardancy; thermal stability

Corresponding Authors: dimitrios.papageorgiou@manchester.ac.uk and ian.kinloch@manchester.ac.uk

1. Introduction

Graphene has attracted the interest of the academic community since its isolation in 2004 due to its unique properties which make it very attractive for use in advanced materials such as polymer nanocomposites [1-5]. However, the industrial scale-up of the production of few layer graphene remains a challenge, restricting its widespread use. Thus, the majority of industrial graphene polymer nanocomposites have to date used either reduced graphene oxide (rGO), multilayer graphene (MLG) or graphene nanoplatelets (GNPs) as reinforcements. In particular, GNPs display similar mechanical, electrical, barrier and thermal properties to few layer graphene but are significantly cheaper to produce and can possess a large aspect ratio and lateral dimension, making them attractive for nanocomposite use [6-12].

One strategy to enhance the properties of a nanocomposite, or counterbalance some of the disadvantages of a specific filler, is the use of hybrid composites where two or more reinforcements are used in combination. Glass fibres (GF) are a conventional reinforcement that is used commonly in polymer matrices due to the fibres' high modulus and low cost [13-16]. Glass fibre reinforced plastics (GFRPs) are used in a number of applications in automotive, aerospace and other industries. However, their disadvantages include high density and poor thermal conductivity and stability. For

the these reasons, in this work we combine both GNPs and GF in order to produce a hybrid composite, that can attribute an additive or synergistic effect on the ultimate properties of the final composite. Pedrazzoli *et al.* [17] have followed the same strategy for the production of mechanically robust polypropylene graphene/glass-fibre composites. The authors observed an increase of interfacial interactions between the matrix and GF due to the presence of GNPs, while increases of around 105% for the modulus and 16% for the tensile strength with the hybrid filler were observed. Moreover, in our previous work [18], we observed additive effects for the modulus of the composites that was three times higher than that of the matrix, while the thermal conductivity of the composites with the hybrid filler, was increased by a factor of five.

In earlier work, Dittrich *et al.* [19] examined the effect of a number of carbonaceous nanoparticles with different geometrical characteristics and degree of exfoliation on the thermal and fire properties of polypropylene. It was found that carbon nanocomposites increased the thermal stability of PP but decreased the time to ignition, while the formation of residue layers during combustion reduced the peak in the heat release rate curves by 74%. Furthermore, previous works on GNP-reinforced polymers have revealed the efficiency of graphene nanoplatelets on the reduction of the peak heat release rate (PHRR), as a result of the effective formation of a protective char, such as in TPU [20], poly(ethylene terephthalate)/polypropylene blends [21], polyethylene/alumina trihydrate composites [22], epoxy [23], polycarbonate/acrylonitrile-butadiene-styrene blends [24] and others. However, ambiguous results have been presented in literature regarding the effect of nanoparticles on the time to ignition (TTI). Schartel and coworkers stated [25] that barrier formation and melt viscosity should not always account for fire retardancy mechanisms in polymer nanocomposites, but additional mechanisms should be evaluated for hybrid systems and combinations of nanoparticles (ie. graphene nanoplatelets) with other fire retardant materials [26-30].

Herein, we have focused on the thermal decomposition and flame retardancy of PP-GF-GNP hybrid composites. The effect of each individual filler along with the hybrid system on the thermal stability

has been evaluated by thermogravimetric analysis (TGA). Understanding the decomposition mechanism aids improving the thermal stability of polymer nanocomposites and thus pyrolysis/gas chromatography/mass spectroscopy was utilized to evaluate the decomposition products. Finally, cone calorimetry was employed to measure the ignition and forced combustion performance of the nanocomposites produced.

2. Experimental

2.1 Materials

Polypropylene homopolymer was provided from Lyondellbasell under the commercial name Moplen HP501L and exhibited a flow index 6 g/10 min and a melt density 900 kg/m^3. The glass-filled polypropylene was provided by ALBIS under the commercial name Altech PP-H A 2020/159 GF20 CP. The material was filled with 20 wt% of E-glass fibres (average length over 5 mm and average diameter of 15 μm) and had a melt density of 1040 kg/m^3. The graphite nanoplatelets (xGNP-M25) were produced by exfoliating sulphuric-based intercalated graphite and were obtained from XG Sciences (East Lansing, MI). The nanoplatelets exhibited a mean platelet diameter of 25 μm and an average thickness of 6-8 nm, according to the supplier. The GNP oxygen content was < 1% and the residual acid content was < 0.5 wt%.

The extrusion process was performed with a twin-screw extruder (Thermo Scientific HAAKE MiniLab micro compounder) at 190 $^{\circ}$C and 100 rpm for 12 minutes. The extrudates were further processed into thin films by hot pressing at 190 °C.

The GNP-filled materials are named PP-GNPx throughout the manuscript, where x is the filler content given in wt% (x= 5, 10, 20 wt%). A similar convention was used for samples filled with GF (PP-GFx). For the production of hybrids, the PP material filled with 20 wt% GF (PP-GF20) was used as a matrix and the GNP were added in the melt mixing process. This caused a dilution of the GF content in the final batch with increasing GNP content, lowering the overall amount of GF. Three set of samples were prepared; PP-GF19-GNP5, PP-GF18-GNP10 and PP-GF16-GNP20.

2.2 Characterization of the PP composites

A TA Q100 differential scanning calorimeter (DSC) from TA Instruments, calibrated with indium and zinc standards, was used to study the crystallization and melting behaviour of the nanocomposites. Dry nitrogen gas was purged into the DSC cell at a flow rate of 50 mL/min. 5 ± 0.2 mg of sample was sealed in an aluminium pan and heated at a rate 10 °C/min to 220 °C, which is above the equilibrium melting point of PP, for 3 minutes. It should be noted that this procedure was followed in order to erase the thermal history of the samples. The samples were then cooled to room temperature at a rate of 10 °C/min and the crystallization peaks were recorded. Finally, the samples were reheated up to 220 °C, in order to obtain the melting temperatures along with the melting enthalpies for the calculation of the respective crystallinities.

Thermogravimetric analysis experiments were carried out using a Setaram Setsys TG-DTA 16/18 instrument. 5±0.5 mg of sample was placed in an alumina crucible and an empty alumina crucible was used as a reference. The samples were heated from room temperature up to 600 °C under a 50 mL min^{-1} flow of N_2 at 10 °C min^{-1}. The sample mass, temperature and heat flow were continuously recorded in order to evaluate the thermal stability of the materials. The onset temperature was defined from the 2% mass loss.

The pyrolysis/gas chromatography/mass spectroscopic (Py/GC/MS) analysis was conducted on the PP and the nanocomposites filled with the maximum content of filler (PP-GNP20, PP-GF20 and PP-GF16-GNP20). A very small amount of the sample (around 1 mg) was placed initially into a sample cup on a Multi-Shot EGA/PY-3030D Pyrolyzer (Frontier Laboratories Ltd., Fukushima, Japan). The sample was then allowed to fall freely into the pyrolyzer furnace. The pre-selected pyrolysis temperatures were 450 and 550 °C and the GC oven temperature was programmed from 50 to 300 °C at 10 °C/min. The sample vapours generated in the furnace were split (in a ratio of 1/50), a portion moved to the column at a flow rate of 1 mL/min and the remaining portion exited the system via the

vent. The pyrolyzates were separated in the Ultra Alloy metal capillary column (UA+5) and analysed by the MS detector GC–MS-QP2010 Ultra (Shimadzu, Japan).

Vertical flammability tests were carried out on compression moulded 80 x 12 x 2 mm^3 specimens by applying a 20 ± 2 mm yellow-tipped blue methane flame to the free end at the lower edge of the bar for 10 s. Prior to the tests, all specimens were conditioned at 23 °C for at least 24 h at 50% relative humidity. In the absence of self-extinguishment, the time at which the flame reaches the clamp was registered, to evaluate the rate of vertical propagation of the flame.

Forced combustion tests were performed on a Cone Calorimeter (FTT, UK) in the horizontal configuration using 50 x 50 x 3 mm^3 specimens prepared by compression moulding. Prior to the tests, the specimens were conditioned at 23 °C for at least 24 h at 50% relative humidity. in a climatic chamber. Tests were performed with a 35 kW/m^2 external heat flux in order to evaluate the fire properties of the composites in conditions comparable to a mild fire scenario [31]. Specimens were wrapped in aluminium foil leaving the upper surface exposed to the radiator and placed on a ceramic backing board at a distance of 25 mm from cone base. All tests were performed at least three times in order to check reproducibility and the averaged curves are reported.

3. Results

3.1 Crystallinity, Crystallization and Melting

In order to study their melting behaviour, the samples were subjected to the standard heating procedure (melting-cooling-remelting) so as to erase their thermal history and obtain their melting temperature and heat of fusion. From the results presented in Supplementary Information (SI) – Figure S3, it can be seen that the melting temperature of all samples were within ± 1 ^oC. The heat of fusion was obtained from the area under the melting curve and the crystallinity was calculated from the well-known equation: $X_c = \frac{\Delta H_m}{\Delta H_m^0}$. The results from the calculations of crystallinity can be seen in Table 1. The heat of fusion and the values of the degree of crystallinity have been normalized by the weight fraction of the matrix, while the heat of fusion for 100% crystalline PP was taken as

$\Delta H_m^0 = 207\ \mathrm{J\ g^{-1}}$ [32]. It can be seen that the samples presented small differences between them. The GNP-filled samples exhibited higher crystallinity than the matrix, while on the contrary, the GF-containing samples displayed lower crystallinity than the matrix. The values are in accordance with the crystallinities obtained by XRD in our previous work [18]. Moreover, the variation of the peak temperature of crystallization, observed in Table 1, indicates the efficiency of GNPs as nucleating agents. For the PP-GNP samples, the presence of the "foreign" substances at high loadings, along with their large surface area, provides a number of sites enabling heterogeneous nucleation at temperatures higher than that of the neat polymer, reaching over 11 ^{o}C for the material with the highest loading. Interestingly, GFs did not facilitate crystallization but retarded the overall phenomenon since the crystallization peaks were detected at temperatures lower than for the matrix. Furthermore, the differences were very small for the specific set of samples, indicating that the volume fraction of glass fibres does not affect significantly the crystallization temperatures. Finally, for the hybrid set of samples, it can be seen that the T_c values are similar to the ones observed for the samples filled only with GNP (PP-GNP), an indication that GFs are acting almost as inert fillers during crystallization, while the strong nucleation characteristics of the GNPs, prevail.

Table 1. Degree of crystallinity and crystallization temperature of all samples under study. The X_c values are accurate to ± 2%, while the T_c values are accurate to ± 1 ^{o}C)

Samples	X_c **(%)**	T_c **(^{o}C)**	**Samples**	X_c **(%)**	T_c **(^{o}C)**	**Samples**	X_c **(%)**	T_c **(^{o}C)**
PP	51.1	119.5	**PP**	51.1	119.5	**PP**	51.1	119.5
PP-GNP5	52.9	126.4	**PP-GF5**	48.9	117.1	**PP-GF19-GNP5**	54.1	127
PP-GNP10	54.2	127.5	**PP-GF10**	48.3	117.2	**PP-GF18-GNP10**	56.4	128.5
PP-GNP20	56.6	130.7	**PP-GF20**	46.7	117.6	**PP-GF16-GNP20**	57.8	130

3.2 Thermogravimetric Analysis

The thermal stability of the composite samples was evaluated by thermogravimetric analysis in nitrogen (Figure 1). As it can be seen in Table 2 for the PP-GNP samples, the presence of GNPs retarded the thermal decomposition significantly for all GNP contents, while the maximum increase of thermal stability occurred when the matrix was reinforced with 10 wt% GNPs, enhancing the onset of decomposition by 48 °C. In contrast, for the PP-GF samples, the presence of glass fibres reduced the thermal stability of the PP matrix, most possibly as a result of weak interactions with the PP matrix - as it was also observed from scanning electron microscopy (SI -Figure S1) - and low aspect ratio, which allows the volatile decomposition products formed, to escape with ease during degradation. Moreover, as was shown in our previous work [18], the GF increase the flexibility of the PP chains, leading to higher mobility during heating and lower activation energy for decomposition. The degree of crystallinity results also point towards this direction, as all PP-GF samples displayed lower crystallinity than the matrix. The material filled with 20 wt% glass fibres showed the highest thermal stability in this set of samples (but still lower than the stability of the matrix).

Finally, for the set of the hybrid samples (PP-GF-GNP), the beginning of thermal decomposition is always observed at higher temperatures than the matrix, as a result of the presence of GNPs. At low GNP content (and higher GF content), the thermal stability is lower than their counterparts filled with GNPs (at the same GNP content), as a result of the presence of GF. Thus, there is a competitive effect between GF and GNP on the decompostion; GFs tend to decrease the thermal stability, whilst GNPs increase it. The effect of GNPs dominates that of the GFs, leading to an overall improvement in performance. The thermal decomposition of the PP-GF16-GNP20 sample was delayed by 57 °C. The geometrical characteristics of GNPs (ie. large aspect ratio and surface area) enhanced greatly the thermal stability of the matrix for both sets of samples that included GNPs, due to the improved interactions (SI - Figure S1c-d), the formation of a tortuous path and the prevention of the emission of gaseous molecules during thermal decomposition.

The results can be also considered with regard to the *nanoconfinement concept* described by Chen *et al.* [33], according to which, the presence of GNPs creates areas where the macromolecular chains of the matrix are confined, disturbing their regular coil conformation and restricting their movement. This phenomenon can also explain the high thermal stability of the hybrid samples, since the simultaneous presence of the GF and the GNP occupy an extensive area in the volume of the hybrid sample, forming a well-distributed filler network and confined even more the movement of the PP macromolecules. The results from DMA [18] also point towards this direction, since the increase of the glass transition temperature for the composite samples indicates that the flexibility of the macromolecular chains of the composite samples is lower than that of neat polymer, therefore contributing to the increase of the thermal stability. In particular, the sample with the highest filler content PP-GF16-GNP20, displays the highest thermal stability, since the GF content is optimum so as to induce a volume exclusion phenomenon and confine the GNPs and the macromolecular chains of the polymer. Moreover, the crystallinity of the specific sample is 7-8% higher than that of the matrix, a fact which should also indicate that the mobility of the polymer chains is restricted.

Table 2. Thermal stability of the samples under nitrogen. All values are accurate to ± 2 ^{o}C.

Samples	$T_{2\%}$ **(^{o}C)**	**Samples**	$T_{2\%}$ **(^{o}C)**	**Samples**	$T_{2\%}$ **(^{o}C)**
PP	360.9	**PP**	360.9	**PP**	360.9
PP-GNP5	390.8	**PP-GF5**	343.2	**PP-GF19-GNP5**	377.6
PP-GNP10	408.8	**PP-GF10**	342.6	**PP-GF18-GNP10**	402
PP-GNP20	406.1	**PP-GF20**	355.2	**PP-GF16-GNP20**	418.4

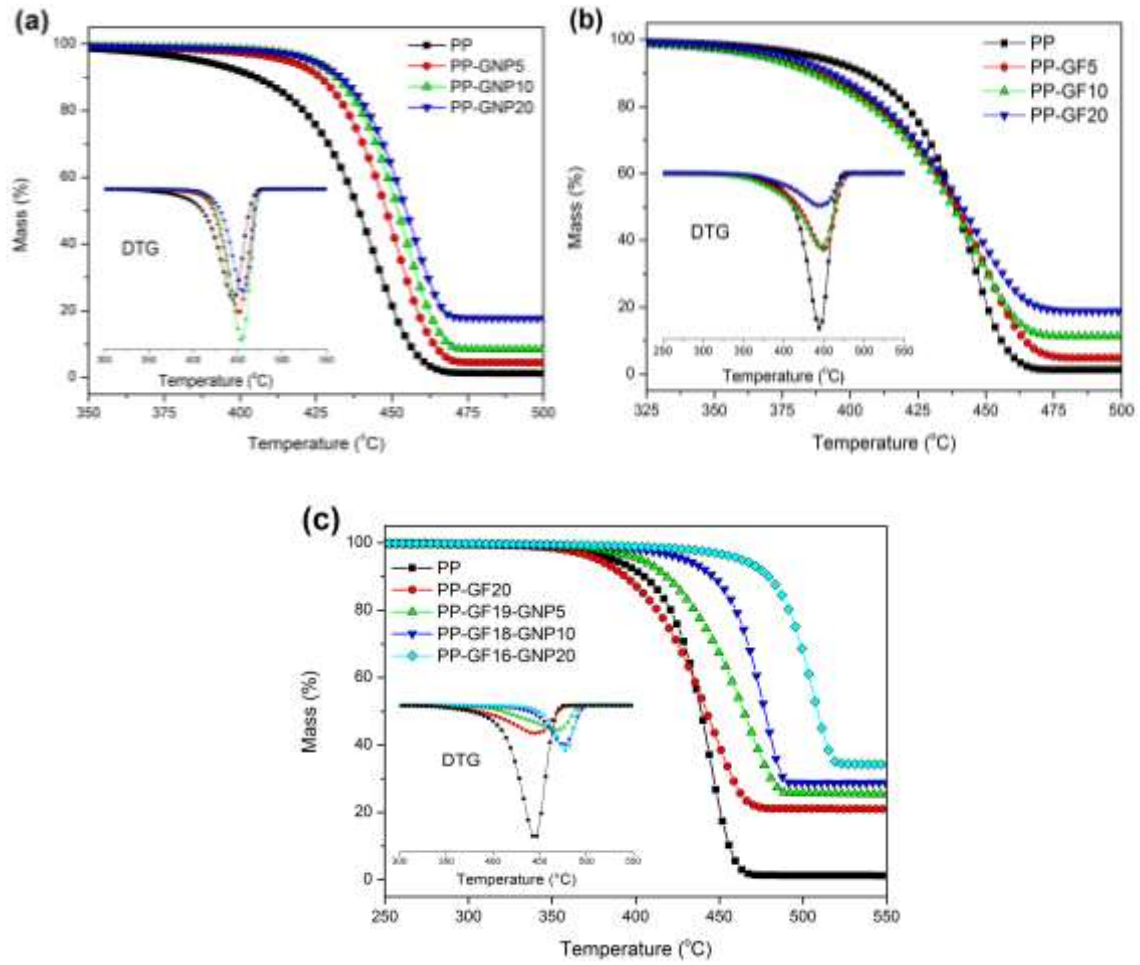

Figure 1. Thermal stability of the three sets of composite samples in nitrogen: (a) PP-GNP, (b) PP-GF, (c) PP-GF-GNP (the insets show the derivative of the mass loss curves)

3.3 Pyrolysis/gas chromatography/mass spectroscopy (Py/GC/MS)

Py/GC/MS can be used to study the specific mechanisms of thermal degradation of polymers in depth. Initially, evolved gas analysis (EGA) was performed with the use of a deactivated tube in the GC oven instead of a capillary column. The EGA thermograms of the samples with the highest amount of fillers are presented in SI - Figure S4. In agreement with the results from TGA measurements, thermal stability is enhanced for the PP-GNP20 and PP-GF16-GNP20 samples. The PP and PP-GF20 samples start releasing pyrolyzates at 350 °C, while PP-GNP20 and PP-GF16-GNP20 start to degrade at higher temperatures (about 450 °C). All samples are completely pyrolyzed at 550 °C. After EGA, the matrix and the composite samples were pyrolyzed in 450 and 550 °C,

temperatures that correspond to the mid-point and the end of degradation, in order to compare the degradation mechanisms of the samples.

Due to the presence of tertiary carbon atoms, PP is susceptible to degradation that occurs by free-radical chain reaction which leads to chain scission. It consists of several steps, including initiation, propagation, chain branching and termination resulting in non-radical product [34]. The resulting chromatographs of PP-GNP20 after pyrolysis at 450 and 550 °C is presented in Figure 2, while those of of PP, PP-GF20 and PP-GF16-GNP20 are presented in SI-Figure S5 (a-c).

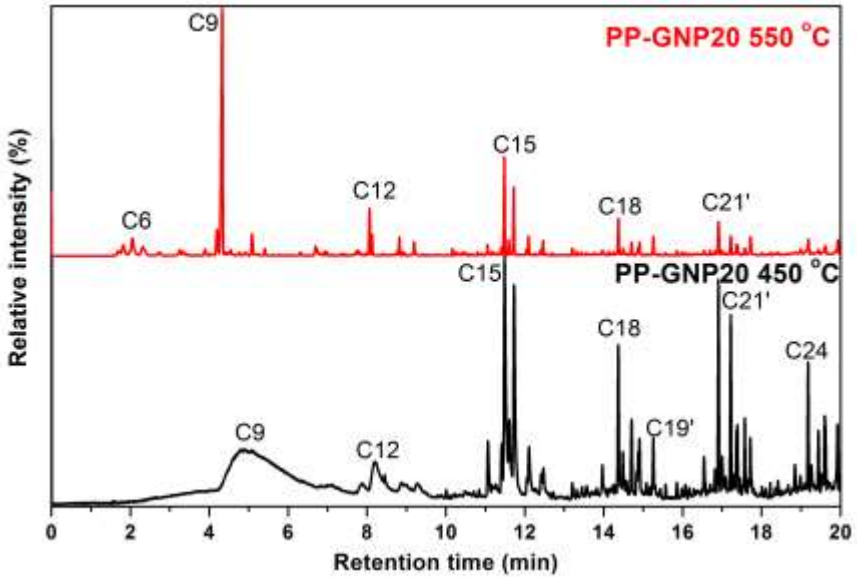

Figure 2. Chromatographs of PP-GNP20, after pyrolysis at 450 °C and 550 °C.

All the degradation products of the PP and the composites are pentane and unsaturated hydrocarbons with the number of carbon atoms ranging from 6 to 25. It is important to note that the absence of the propylene monomer from the chromatographic patterns can be attributed to the fact that the MS detector was set to collect mass spectra of compounds with molecular weights greater than 50, in order to avoid additional peaks of gases like CO and CO_2. When pyrolyzed at lower temperatures, the resulting products are mostly oligomers with a large number of carbon atoms, while increased temperature (550 °C) results in pronounced degradation leading to the formation of greater quantities of low molecular weight products, such as C9. Compounds with greater molecular weight require more energy to diffuse though the polymer matrix, so their evolution is more difficult

at lower pyrolysis temperatures. The identified pyrolysis products are presented in the SI - Table S1-S4. Peak areas (%) were calculated with respect to the sum of all areas of the identified products. All samples released the same degradation products; hence the GF and GNP did not affect the decomposition mechanism of the PP. The enhanced thermal stability is thus due to the barrier effect the fillers provide and therefore the prevention of the emission of gaseous molecules, as well as the restriction of the movement of the macromolecular chains as a result of nanoconfinement. The chromatographs exhibit complex patterns with a number of peaks, as a result of random chain scission. Breaking of the C-C bonds results in primary and secondary radicals, with the formation of the latter being favoured since it is more stable and yields the major decomposition products. Secondary radicals can also become saturated via intramolecular hydrogen transfer and yield n-pentane. Intramolecular transfer of the secondary terminal radicals to tertiary hydrogen atoms and subsequent β-scission results in the formation of oligomeric 1-alkene products with 3n carbon atoms (C6, C9, C12, C15 etc.), and finally isomerization due to the branched structure of PP that results in the production of various stereoisomers as pyrolysis products [35, 36]. Primary radicals are also subjected to intramolecular transfer to carbon atoms at the 4-, 6- and 8- positions, resulting in minor degradation products with carbon numbers 3n+1 (C10, C12, C16 etc). The mechanism of degradation of PP is depicted in Scheme 1. Finally, the identified alkadienes can be produced by terminally-unsaturated polymeric chains subjected to intermolecular radical transfer [35].

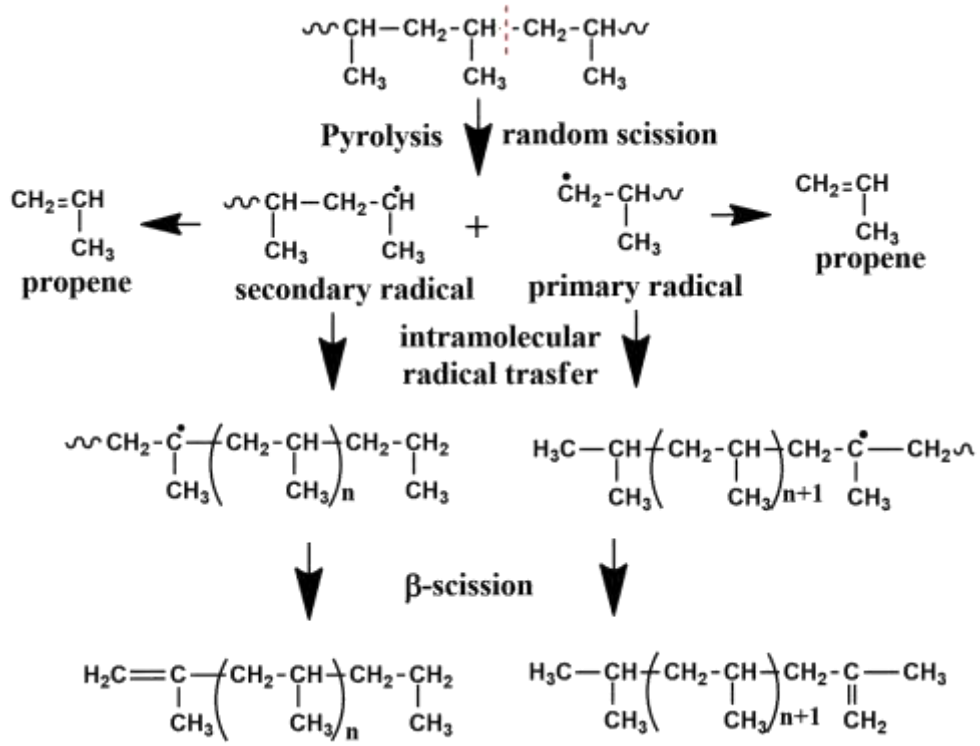

Scheme 1. Thermal degradation mechanism of PP

The effect of pyrolysis temperature on the relative variation of the pyrolysis products is presented in Figure 3. The percentage composition of n-pentane (C5), alkenes derived from primary and secondary radicals and finally alkadienes were calculated in respect to the total % relative areas of the released products. As temperature increases, the production of alkenes with number of carbon atoms 3n is more pronounced in all samples, indicating they are the major degradation products at both temperatures. This confirms the formation of mainly secondary radicals during degradation. The presence of GNP20 and GF16-GNP20 in the PP matrix reduces the relative amount of 3n pyrolysis products compared with pure PP and PP-GF20, confirming that both GNP as well as the combination of GNP and GF enhance the thermal stability of PP by hindering the formation and diffusion mainly of secondary radicals, that are the main products of C-C radical scission of the polymer.

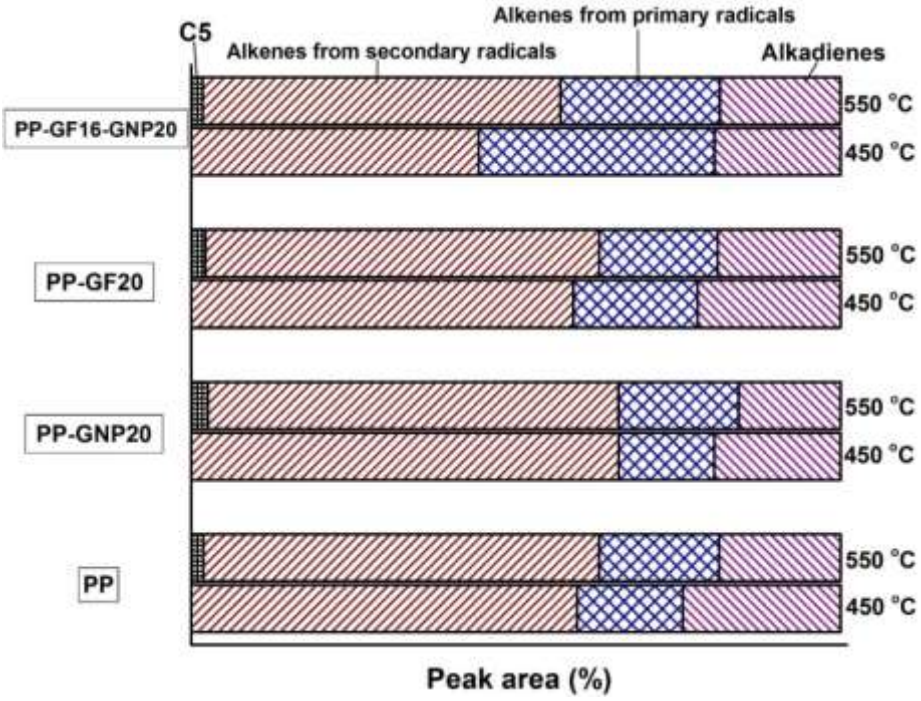

Figure 3. Variation in the composition of the pyrolyzate of PP and its composites

3.4 Flammability and Forced Combustion

The flammability of the nanocomposites was evaluated by vertical flammability tests and the results were compared to pristine PP. As expected, the polypropylene matrix exhibited a rapid and complete combustion, along with extensive dripping from the specimens. The introduction of GNP, GF or their combination did not result in a significant reduction of the PP flammability, as no self-extinguishment was observed for the composites and dripping occurred except for the PP-GF16-GNP20 sample, which produces a stable char during the test. However, an increase was observed in the time to reach the clamp for the GNP-based nanocomposites (SI – Table S5), suggesting a reduction of the combustion rate in the presence of nanoparticles. Similar results were observed previously for polymer nanocomposites [37] and they are related to the fact that in the specific conditions, the accumulation of nanoparticles upon polymer ablation is affected by the molten polymer flow, producing physical defects in the protecting layer and thus strongly reducing its effectiveness. However, the accumulation of nanoparticles during combustion was previously reported to deliver strong reductions in the rate of forced combustions. The experimental results

from the cone calorimetry tests for PP and the corresponding composites filled with GNP, GF and the hybrid GF-GNP are presented in Figure 4 and Table 4. The heat release rate plot for pure PP (Figure 4) is typical of a highly flammable non-charring material, exhibiting a complete polymer volatilization and rapid combustion, yielding a peak heat release rate (PHRR) at 1140 ± 150 kW/m^2 and flameout at about 198 ± 15 s.

The introduction of the GNPs altered the phenomenology during polymer combustion, leading to the production of a solid char, which affects the shape of the HRR curves and reduces the PHRR to more than half at 10% GNP content. As the heat of combustion is released at a much lower rate, the contribution of PP/GNP nanocomposites to the growth of a developing fire is significantly lower than for pristine PP, with obvious benefits in real fire scenarios. On the other hand, GFs had almost no effect in terms of surface charring, despite the obvious accumulation of glass fibres as a consequence of polymer ablation, and determined no significant difference in neither the shape of the heat release rate plot nor the PHRR. Indeed, the formation of a solid, compact and continuous char during polymer nanocomposites combustion is a well-known effect of well dispersed high aspect ratio nanoparticles. The presence of GNPs enabled the formation of a carbonaceous protective layer obtained as a consequence of polymer ablation and accumulation of GNPs, acting as a barrier layer to heat and mass transfer [19], which slows down the overall combustion process.

Kashiwagi *et al.* [38] have shown for the case of single-walled carbon nanotubes, that the homogeneous dispersion of the fillers is vital in order to obtain a high-quality protective layer of residue in nanocomposites. In this case, the sample filled with 10 wt% GNPs presented the optimal filler density so as to form a well-organized percolation network that is crucial for the formation of the protective char layer throughout the volume of the sample. It is worth noting that higher GNP content does not appear to be beneficial as the nanocomposite containing 20 wt% GNPs exhibited a higher combustion rate. This may be due to foreseen aggregation of the GNPs at the highest loading or to the formation of a very stiff network during combustion, causing local defectiveness in the barrier layer. GNPs are also effective in promoting char forming in the presence of GFs, as it can be

clearly observed by the rate obtained for the PP-GF19-GNP5 and PP-GF18-GNP10 samples. Beside the clear reduction of heat release rate, an important result is that total smoke released upon combustion is not significantly affected by the presence of GNPs, which is an important advantage compared to conventional flame retardants, which often increase the smoke optical density, this representing a severe hazard in the event of fire.

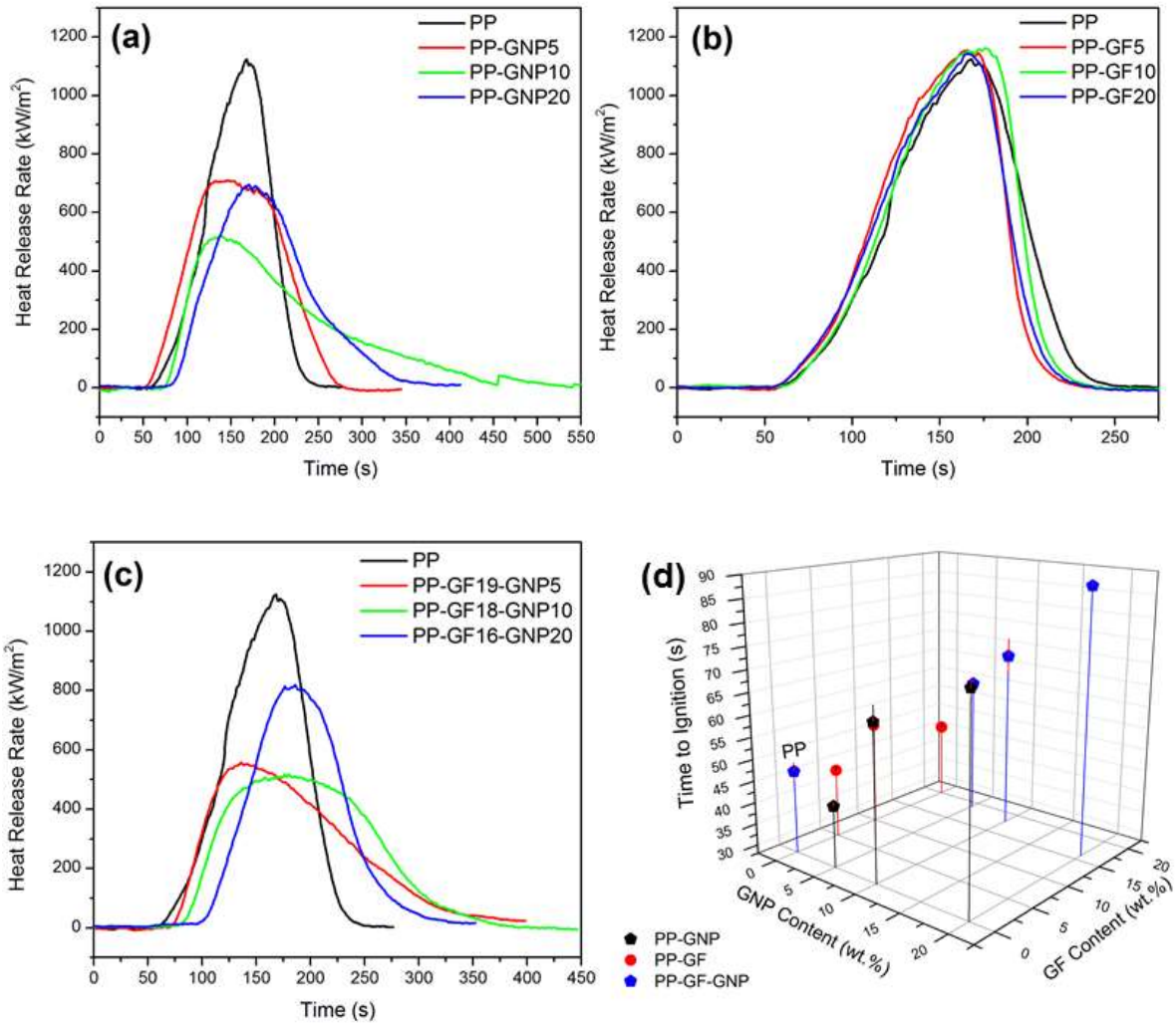

Figure 4. (a,b,c) Heat release rate curves of PP and nanocomposites filled with GNP, GF and GF-GNP, (d) time to ignition for all samples under study.

An interesting observation came from the study of the results of the time to ignition (TTI) for the PP and nanocomposites, presented in Table 4. While the presence of GFs did not attribute any significant changes to the TTI, the presence of GNPs at loadings ≥10 wt% or in combination

with GFs, resulted in a delayed ignition of the composite samples. This fact is of particular interest as nanocomposites have most often been reported to ignite earlier than pristine polymers [19, 39, 40]. The TTI of polymers depends on an interplay of different phenomena, including heat transfer (absorption, reflection and transmission) controlling heating of the polymer, decomposition reactions determining the production of volatile fuel as well as mass transfer (diffusion, adsorption) of volatiles to the atmosphere, where a minimum concentration has to be reached in order to allow the establishment of a sustained flame. The presence of GNPs may clearly affect several of the chemical and physical parameters controlling the ignition, including radiative absorption/emission parameters, thermal conductivity, heat capacity and viscosity of the molten phase. Furthermore, at relatively high inorganic loading (e.g. >20%), a delay towards higher TTI may be expected, simply related to the lower amount of polymer available for the production of volatile fuel. This may explain, for instance, why TTI for PP-GF16-GNP20 is higher than PP-GNP20. However, a complete description of the phenomena explaining the TTI delay would require extensive characterization of these parameters during the pre-ignition phase, which is beyond the scope of this work.

Table 4. Heat release rate (HRR), peak heat release rate (PHRR) and time to ignition (TTI) for all samples under study.

Samples	**HRR (kW/m^2)**	**PHRR (kW/m^2)**	**TSR (-)**	**TTI (s)**
PP	391 ± 18	1140 ± 153	1636 ± 89	49 ± 5
PP-GNP5	311 ± 7	724 ± 25	1855 ± 53	42 ± 1
PP-GNP10	212 ± 24	520 ± 15	1675 ± 73	63 ± 3
PP-GNP20	267 ± 5	697 ± 19	1715 ± 66	76 ± 8
PP-GF5	387 ± 32	1165 ± 76	1528 ± 14	44 ± 1
PP-GF10	420 ± 8	1177 ± 30	1576 ± 19	52 ± 5
PP-GF20	376 ± 5	1155 ± 5	1515 ± 17	46 ± 1

PP-GF19-GNP5	265 ± 20	563 ± 13	1806 ± 45	60 ± 1
PP-GF18-GNP10	241 ±24	522 ± 11	1606 ± 40	69 ± 4
PP-GF16-GNP20	301 ± 25	826 ± 47	1407 ± 84	88 ± 1

4. Conclusions

The effect of the presence of GNPs and GFs both individually and simultaneously on the thermal and fire properties of polypropylene, was investigated. The presence of GNPs enabled a significant increase of the thermal stability of the samples as a result of their high inherent thermal stability and good dispersion within the matrix that enabled a nanoconfinement effect to the macromolecular chains of PP and prevented the escape of the gaseous molecules with increasing temperature. Glass fibres on the other hand, did not contribute to the increase of the thermal stability and reduced slightly the thermal stability of the matrix. The activation energy needed to break down the primary and secondary radicals of the matrix was dependent on the thermal stability of each material as it was shown by the pyrolysis/gas chromatography/mass spectroscopy results. Moreover, from Py/GC/MS it was found that the alkenes with number of carbon atoms of 3n were the main degradation products for all samples. Finally, the cone calorimetry tests revealed that GNPs altered the phenomenology during combustion, which led to the formation of a char and also formed an active carbonaceous layer that acted as a barrier layer during heat and mass transfer. In conclusion, the easily-produced GNP-based composite materials can be used in a number of advanced applications where good mechanical performance [18] is needed, alongside high thermal stability.

Associated Content: Supplementary Information including SEM images, comparative TGA graphs for the 3 set of samples, melting curves of all samples, EGA chromatographs of PP and nanocomposites, chromatographs of 4 samples after pyrolysis at 450 °C and 550 °C and the respective pyrolysis product tables can be found online.

Acknowledgements

This research has been supported by funding from the European Union Seventh Framework Programme under grant agreement no 604391 Graphene Flagship and the EPSRC (award no. EP/I023879/1). The authors are grateful to Albis UK Ltd for the supply of polypropylene materials and helpful discussions.

References

[1] D.G. Papageorgiou, I.A. Kinloch, R.J. Young, Mechanical properties of graphene and graphene-based nanocomposites, Progress in Materials Science 90 (2017) 75-127.

[2] J.R. Potts, D.R. Dreyer, C.W. Bielawski, R.S. Ruoff, Graphene-based polymer nanocomposites, Polymer 52(1) (2011) 5-25.

[3] D.G. Papageorgiou, I.A. Kinloch, R.J. Young, Graphene/elastomer nanocomposites, Carbon 95 (2015) 460-484.

[4] H. Kim, A.A. Abdala, C.W. Macosko, Graphene/Polymer Nanocomposites, Macromolecules 43(16) (2010) 6515-6530.

[5] R.J. Young, I.A. Kinloch, L. Gong, K.S. Novoselov, The mechanics of graphene nanocomposites: a review, Composites Science and Technology 72(12) (2012) 1459-1476.

[6] S. Li, Z. Li, T.L. Burnett, T.J.A. Slater, T. Hashimoto, R.J. Young, Nanocomposites of graphene nanoplatelets in natural rubber: microstructure and mechanisms of reinforcement, Journal of Materials Science 52(16) (2017) 9558-9572.

[7] C. Vallés, A.M. Abdelkader, R.J. Young, I.A. Kinloch, The effect of flake diameter on the reinforcement of few-layer graphene–PMMA composites, Composites Science and Technology 111 (2015) 17-22.

[8] H.-B. Zhang, W.-G. Zheng, Q. Yan, Y. Yang, J.-W. Wang, Z.-H. Lu, G.-Y. Ji, Z.-Z. Yu, Electrically conductive polyethylene terephthalate/graphene nanocomposites prepared by melt compounding, Polymer 51(5) (2010) 1191-1196.

[9] S. Quiles-Díaz, P. Enrique-Jimenez, D.G. Papageorgiou, F. Ania, A. Flores, I.A. Kinloch, M.A. Gómez-Fatou, R.J. Young, H.J. Salavagione, Influence of the chemical functionalization of graphene on the properties of polypropylene-based nanocomposites, Composites Part A: Applied Science and Manufacturing 100 (2017) 31-39.

[10] M.A. Rafiee, J. Rafiee, Z. Wang, H. Song, Z.-Z. Yu, N. Koratkar, Enhanced Mechanical Properties of Nanocomposites at Low Graphene Content, ACS Nano 3(12) (2009) 3884-3890.

[11] K. Kalaitzidou, H. Fukushima, L.T. Drzal, Multifunctional polypropylene composites produced by incorporation of exfoliated graphite nanoplatelets, Carbon 45(7) (2007) 1446-1452.

[12] K. Kalaitzidou, H. Fukushima, L.T. Drzal, Mechanical properties and morphological characterization of exfoliated graphite–polypropylene nanocomposites, Composites Part A: Applied Science and Manufacturing 38(7) (2007) 1675-1682.

[13] J. Thomason, M. Vlug, Influence of fibre length and concentration on the properties of glass fibre-reinforced polypropylene: 1. Tensile and flexural modulus, Composites Part A: Applied Science and Manufacturing 27(6) (1996) 477-484.

[14] S.-L. Gao, E. Mäder, Characterisation of interphase nanoscale property variations in glass fibre reinforced polypropylene and epoxy resin composites, Composites Part A: Applied Science and Manufacturing 33(4) (2002) 559-576.

[15] M. Van den Oever, T. Peijs, Continuous-glass-fibre-reinforced polypropylene composites II. Influence of maleic-anhydride modified polypropylene on fatigue behaviour, Composites Part A: Applied Science and Manufacturing 29(3) (1998) 227-239.

[16] M. Sanjay, G. Arpitha, B. Yogesha, Study on mechanical properties of natural-glass fibre reinforced polymer hybrid composites: A review, Materials today: proceedings 2(4-5) (2015) 2959-2967.

[17] D. Pedrazzoli, A. Pegoretti, K. Kalaitzidou, Synergistic effect of graphite nanoplatelets and glass fibers in polypropylene composites, Journal of Applied Polymer Science 132(12) (2015) 41682.

[18] D.G. Papageorgiou, I.A. Kinloch, R.J. Young, Hybrid multifunctional graphene/glass-fibre polypropylene composites, Composites Science and Technology 137 (2016) 44-51.

[19] B. Dittrich, K.-A. Wartig, D. Hofmann, R. Mülhaupt, B. Schartel, Flame retardancy through carbon nanomaterials Carbon black, multiwall nanotubes, expanded graphite, multi-layer graphene and graphene in polypropylene, Polymer Degradation and Stability 98(8) (2013) 1495-1505.

[20] H. Quan, B.-q. Zhang, Q. Zhao, R.K.K. Yuen, R.K.Y. Li, Facile preparation and thermal degradation studies of graphite nanoplatelets filled thermoplastic polyurethane nanocomposites, Composites Part A: Applied Science and Manufacturing 40(9) (2009) 1506-1513.

[21] I.M. Inuwa, A. Hassan, D.-Y. Wang, S.A. Samsudin, M.K. Mohamad Haafiz, S.L. Wong, M. Jawaid, Influence of exfoliated graphite nanoplatelets on the flammability and thermal properties of polyethylene terephthalate/polypropylene nanocomposites, Polymer Degradation and Stability 110 (2014) 137-148.

[22] Z. Han, Y. Wang, W. Dong, P. Wang, Enhanced fire retardancy of polyethylene/alumina trihydrate composites by graphene nanoplatelets, Materials Letters 128 (2014) 275-278.

[23] Y. Guo, C. Bao, L. Song, B. Yuan, Y. Hu, In Situ Polymerization of Graphene, Graphite Oxide, and Functionalized Graphite Oxide into Epoxy Resin and Comparison Study of On-the-Flame Behavior, Industrial & Engineering Chemistry Research 50(13) (2011) 7772-7783.

[24] R. Heidar Pour, M. Soheilmoghaddam, A. Hassan, S. Bourbigot, Flammability and thermal properties of polycarbonate /acrylonitrile-butadiene-styrene nanocomposites reinforced with multilayer graphene, Polymer Degradation and Stability 120 (2015) 88-97.

[25] B. Schartel, M. Bartholmai, U. Knoll, Some comments on the main fire retardancy mechanisms in polymer nanocomposites, Polymers for Advanced Technologies 17(9-10) (2006) 772-777.

[26] X. Wang, S. Zhou, W. Xing, B. Yu, X. Feng, L. Song, Y. Hu, Self-assembly of Ni-Fe layered double hydroxide/graphene hybrids for reducing fire hazard in epoxy composites, Journal of Materials Chemistry A 1(13) (2013) 4383-4390.

[27] J. Zhuge, J. Gou, C. Ibeh, Flame resistant performance of nanocomposites coated with exfoliated graphite nanoplatelets/carbon nanofiber hybrid nanopapers, Fire and Materials 36(4) (2012) 241-253.

[28] X. Wang, W. Xing, X. Feng, B. Yu, H. Lu, L. Song, Y. Hu, The effect of metal oxide decorated graphene hybrids on the improved thermal stability and the reduced smoke toxicity in epoxy resins, Chemical Engineering Journal 250 (2014) 214-221.

[29] J. Gu, C. Liang, X. Zhao, B. Gan, H. Qiu, Y. Guo, X. Yang, Q. Zhang, D.-Y. Wang, Highly thermally conductive flame-retardant epoxy nanocomposites with reduced ignitability and excellent electrical conductivities, Composites Science and Technology 139 (2017) 83-89.

[30] D. Hofmann, K.-A. Wartig, R. Thomann, B. Dittrich, B. Schartel, R. Mülhaupt, Functionalized Graphene and Carbon Materials as Additives for Melt-Extruded Flame Retardant Polypropylene, Macromolecular Materials and Engineering 298(12) (2013) 1322-1334.

[31] V. Babrauskas, Specimen heat fluxes for bench-scale heat release rate testing, Fire and Materials 19(6) (1995) 243-252.

[32] S. Boncel, J. Górka, M.S.P. Shaffer, K.K.K. Koziol, Shear-induced crystallisation of molten isotactic polypropylene within the intertube channels of aligned multi-wall carbon nanotube arrays towards structurally controlled composites, Mater. Lett. 116 (2014) 53-56.

[33] K. Chen, C.A. Wilkie, S. Vyazovkin, Nanoconfinement revealed in degradation and relaxation studies of two structurally different polystyrene-clay systems, J. Phys. Chem. B 111(44) (2007) 12685-12692.

[34] S.H. Hamid, Handbook of polymer degradation, Ed. Techniques Ingénieur2000.

[35] E. Jakab, G. Varhegyi, O. Faix, Thermal decomposition of polypropylene in the presence of wood-derived materials, Journal of Analytical and Applied Pyrolysis 56(2) (2000) 273-285.

[36] M.S.P. De Amorim, C. Comel, P. Vermande, Pyrolysis of polypropylene: I. Identification of compounds and degradation reactions, Journal of Analytical and Applied Pyrolysis 4(1) (1982) 73-81.

[37] A. Fina, S. Bocchini, G. Camino, Thermal behavior of nanocomposites and fire testing performance, in: C. W. Wilkie, A. B. Morgan, G. L. Nelson (Eds.), Fire and Polymers V – Materials and Concepts for Fire Retardancy, ACS Publications, USA, 2009, pp. 10-24.

[38] T. Kashiwagi, F. Du, K.I. Winey, K.M. Groth, J.R. Shields, S.P. Bellayer, H. Kim, J.F. Douglas, Flammability properties of polymer nanocomposites with single-walled carbon nanotubes: effects of nanotube dispersion and concentration, Polymer 46(2) (2005) 471-481.

[39] A. Fina, F. Cuttica, G. Camino, Ignition of polypropylene/montmorillonite nanocomposites, Polymer Degradation and Stability 97(12) (2012) 2619-2626.

[40] A. Fina, G. Camino, Ignition mechanisms in polymers and polymer nanocomposites, Polymers for Advanced Technologies 22(7) (2011) 1147-1155.